Supporting Information

Complete reference 56

The complete reference 56 of the main journal text to the Gaussian03 program suite is given as reference 1 below.

Stereo view of the active site

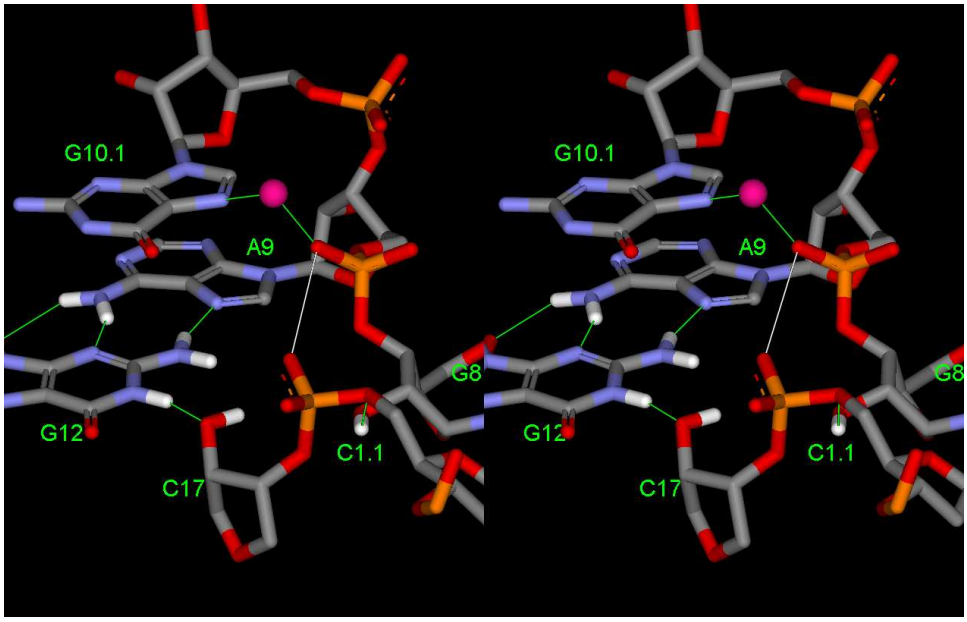

Figure S1: Stereo view of the active site with with Mg^{2+} ion at the C-site position. Green lines are hydrogen bonds or Mg^{2+} coordination with active site residues. The white line connects the A9 and scissile phosphate oxygens. The bridging position of Mg^{2+}, mentioned in the text, is at the middle of the white line.

Methods

Transition state mimics set up

The early TS mimic is close to an ideal phosphorane in that the bond lengths to the endocyclic 2'O and exocyclic 5'O are roughly equal. Density-functional studies of model transesterification reactions suggest that the rate-controlling transition state for a dianionic mechanism are "late" in that the bond to the nucleophile is almost fully formed and shorter whereas the bond to the leaving group is almost completely cleaved and significantly longer with more accumulated charge on the oxygen. A late transition state also avoids typical phosphorane conformational rearrangements (such as pseudorotation) due to the lack of long-lived intermediates along the transesterification reaction,[2] thus allowing us to create MM transition state mimics. The parameters used for the late transition state mimic involved a minor modification of the early transition state mimic.[3] The late TS mimic has nucleophilic P-$O_{2'}$ and leaving group P-$O_{5'}$ bond lengths of 1.856 and 2.382 Å, respectively, and the formal partial charge on the leaving $O_{5'}$ atom was increased from -0.68e to -0.90e while the charge of $C_{5'}$ was adjusted in compensation to ensure overall charge conservation. The modifications for the late transition state mimic were based on density-functional calculations of the rate-controlling transition state for the transesterification reaction of a sugar-phosphate with methoxide leaving group reported previously[4] and available in the QCRNA database.[5]

Equilibration Protocol

The following equilibration procedures (total 1 ns) were applied to the system prior the production simulations in order to insure reasonable relaxation of the solvent and ion environment. The positions of the solute atoms, including the Mg^{2+} ion, were held fixed in the equilibration stages.

Pre-annealing Stage. Water and ion molecules were first energy-optimized then underwent a constant volume simulation annealing for 50 ps. The temperature was increased from 0 K to 298 K in a 7.5 ps period then was kept at 298 K. The annealing simulation were repeated twice with temperature increased from 298 K to 498 K and then back to 298 K.

Annealing Stage. Four steps of constant volume simulations (50 ps each) were performed in the this stage. First step: The temperature increased from 298 K to 498 K in 7.5 ps then was kept at 498 K. Second step: The temperature increased from 498 K to 698 K in 7.5 ps then was kept at 698 K. Third step: The temperature decreased from 698 K to 498 K in 7.5 ps then was kept at 498 K. Fourth step: The temperature decreased from 498 K to 298 K in 7.5 ps then was kept at 298 K. The whole annealing stage was repeated three times before the post-annealing stage.

Post-annealing Stage. Three steps of constant volume simulations were performed in the this stage. First step (50 ps) : The temperature increased from 298 K to 498 K in 7.5 ps then was kept at 498 K. Second step (50 ps) : The temperature decreased from 498 K to 298 K in 7.5 ps then was kept at 298 K. Third step (150 ps): The temperature was kept at 298 K for 150 ps.

Solute Relaxation Stage. The solute atoms were energy-optimized and then were allowed to move under harmonic restraints over a 50 ps simulation at 298 K under constant pressure of 1 atm. The harmonic force constant (in kcal mol^{-1} Å^{-2}) on each heavy atom was obtained from the empirical formula $k_i = 25 + 2{\times}10^3/B_i$ where k_i is the force constant for atom i and B_i is the corresponding crystallographic B-value. The restraints were exponentially released over 50 ps with a half-life decay parameter of 10 ps. At the end of the 50 ps simulation, the restraints were reduced to about 3 percent of the initial restraint values. Three harmonic restraints of 20 kcal mol^{-1} Å^{-2} were added to keep the Mg^{2+} ion in the middle of the C1.1:O_{P2} and A9:O_{P2} positions. Another harmonic restraint of 20 kcal mol^{-1} Å^{-2} was used to force the distance between G8:H_{OP2} and C1.1:O_{P5} to be around 1.8 Å, which is to ensure that the H_{OP2} of G8 is

initially hydrogen bonded. All restraints were then released prior to the production simulation.

Production Simulation. After the 1 ns of solvent equilibration, the whole system was energy-optimized and unconstrained dynamics simulation began from 0 K under constant pressure of 1 atm. The temperature was increased to 298 K at the rate of 1 K/ps and then kept fixed at 298 K. The same equilibration process was applied for each simulation. A total of 12 ns of unconstrained dynamics was performed for each of the eight simulations (reactant with and without Mg^{2+}, early TS mimic and late TS mimic), the last 10 ns of which were used for analysis. The motions and relaxation of solvent and counterions are notoriously slow to converge in nucleic acid simulations,[6] and careful equilibration is critical for reliable simulations. In summary, for each simulation, a total of 3 ns of equilibration (1 ns of solvent relaxation and 2 ns of solvent and structure relaxation) has been carried out before 10 ns of data sampling.

RMSD results

The heavy-atom root-mean-square deviation (RMSD) plots of the entire hammerhead RNA and of the active site residues with respect to the crystallographic structure[7] are shown in Figure S2 for the simulations with Mg^{2+} at the bridging position and the simulation without Mg^{2+}, and in Figure S3 for the simulations with Mg^{2+} initially placed at the C-site position.

Computational resources

Computational resources were provided by the Minnesota Supercomputing Institute with the allocation on a cluster consisting with SGI Altix SMP machines (with total 426 1.5Ghz Intel Itanium-2 CPUs) and an IBM Blade Linux cluster with 1,236 2.6Ghz AMD opteron cores, and by a generous allocation on an IBM Blue Gene BG/L with 4,096 700Mhz CPUs at the On-Demand Center in Rochester, Minnesota with further thanks to Carlos Sosa, Cindy Mestad, Steven Westerbeck, and Geoffrey Costigan for technical assistance. This research was also performed in part using the Molecular Science Computing Facility (MSCF) (with an HP Linux cluster with 1,920 1.5Ghz Intel Itanium-2 CPUs) in the William R. Wiley Environmental Molecular Sciences Laboratory, a national scientific user facility sponsored by the U.S. Department of Energy's Office of Biological and Environmental Research and located at the Pacific Northwest National Laboratory, operated for the Department of Energy by Battelle.

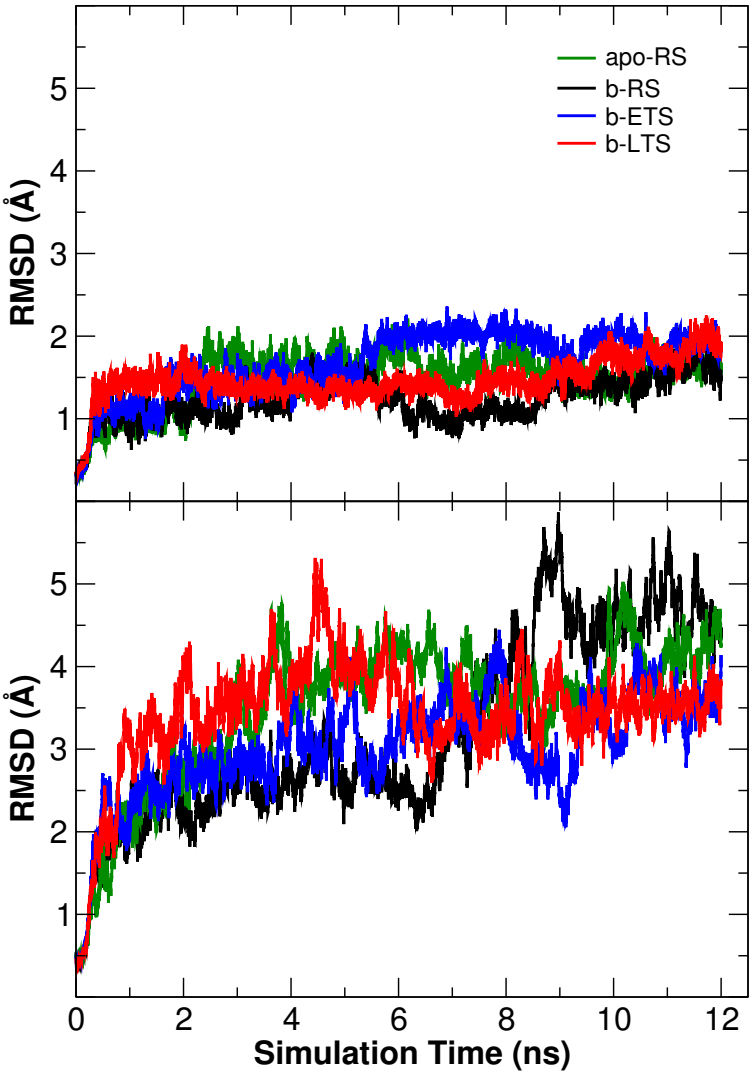

Figure S2: Heavy-atom root-mean-square deviation (RMSD) plots of the active site residues (top) and the whole full length hammerhead system with Mg^{2+} ion at the bridging position (bottom) with respect to the crystallographic structure.[7] The active site was defined as all residues within 10 Å from the scissile phosphate.

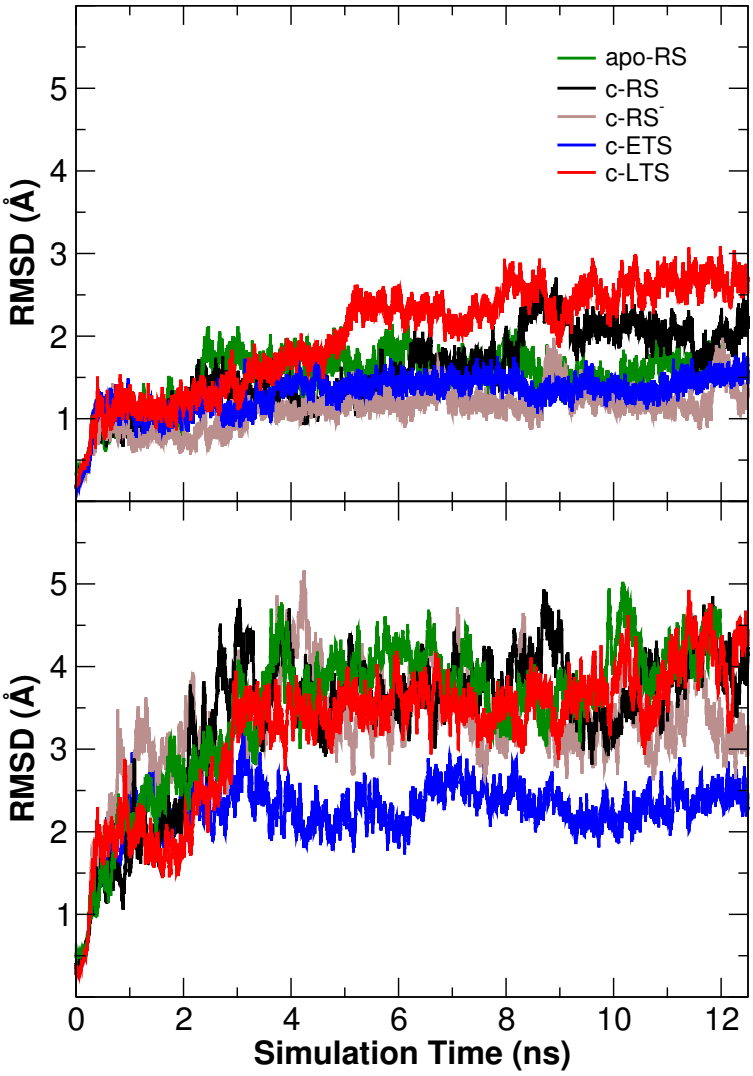

Figure S3: Heavy-atom root-mean-square deviation (RMSD) plots of the active site residues (top) and the whole full length hammerhead system with Mg^{2+} ion at the C-site position (bottom) with respect to the crystallographic structure.[7] The active site was defined as all residues within 10 Å from the scissile phosphate.

Key distances in QM/MM simulations

	b-ETS	b-ETSQM	b-LTS	b-LTSQM
Active site RMSD	1.79(26)	1.32(09)	1.49(22)	1.27(16)
Mg $\cdots$ G8:$O_{2'}$	2.24(13)	2.14(09)	3.21(23)	2.19(22)
Mg $\cdots$ C1.1:$O_{5'}$	3.68(35)	3.95(22)	2.09(05)	2.30(16)
G8:$H_{O_{2'}}$ $\cdots$ C1.1:$O_{5'}$	5.09(74)	3.19(32)	2.36(42)	1.22(39)
G12:N1 $\cdots$ C17:$O_{2'}$	3.14(28)	4.24(40)	2.97(13)	3.37(31)
A9:N6 $\cdots$ G12:N3	3.15(21)	3.08(17)	3.17(21)	3.06(14)
A9:N6 $\cdots$ G12:$O_{2'}$	3.01(18)	3.02(16)	2.99(16)	3.02(16)
A9:N7 $\cdots$ G12:N2	3.85(44)	3.00(14)	3.66(33)	3.04(15)

Table S1: Key distances (Å) in the hammerhead active site from early transition state and late transition state mimics from molecular dynamics (MD) and combined quantum mechanics and molecular mechanics (QM/MM) simulations.[‡]

[‡]The active site is defined as all residues within 10 Å from the scissile phosphate.

[¶]The results for MD simulations were calculated over the last 10 ns with data collected every 1 ps. The QM/MM results were calculated over 1 ns with data collected every 0.5 ps. Entries shown are average values and standard deviations in parenthesis (divided by the decimal precision).

References

(1) FRISCH, M. J., TRUCKS, G. W., SCHLEGEL, H. B., SCUSERIA, G. E., ROBB, M. A., CHEESEMAN, J. R., MONTGOMERY, J. A., JR., VREVEN, T., KUDIN, K. N., BURANT, J. C., MILLAM, J. M., IYENGAR, S. S., TOMASI, J., BARONE, V., MENNUCCI, B., COSSI, M., SCALMANI, G., REGA, N., PETERSSON, G. A., NAKATSUJI, H., HADA, M., EHARA, M., TOYOTA, K., FUKUDA, R., HASEGAWA, J., ISHIDA, M., NAKAJIMA, T., HONDA, Y., KITAO, O., NAKAI, H., KLENE, M., LI, X., KNOX, J. E., HRATCHIAN, H. P., CROSS, J. B., BAKKEN, V., ADAMO, C., JARAMILLO, J., GOMPERTS, R., STRATMANN, R. E., YAZYEV, O., AUSTIN, A. J., CAMMI, R., POMELLI, C., OCHTERSKI, J. W., AYALA, P. Y., MOROKUMA, K., VOTH, G. A., SALVADOR, P., DANNENBERG, J. J., ZAKRZEWSKI, V. G., DAPPRICH, S., DANIELS, A. D., STRAIN, M. C., FARKAS, O., MALICK, D. K., RABUCK, A. D., RAGHAVACHARI, K., FORESMAN, J. B., ORTIZ, J. V., CUI, Q., BABOUL, A. G., CLIFFORD, S., CIOSLOWSKI, J., STEFANOV, B. B., LIU, G., LIASHENKO, A., PISKORZ, P., KOMAROMI, I., MARTIN, R. L., FOX, D. J., KEITH, T., AL-LAHAM, M. A., PENG, C. Y., NANAYAKKARA, A., CHALLACOMBE, M., GILL, P. M. W., JOHNSON, B., CHEN, W., WONG, M. W., GONZALEZ, C., AND POPLE, J. A. Gaussian 03, Revision C.02. Gaussian, Inc., Wallingford, CT, 2004.

(2) LÓPEZ, C. S., FAZA, O. N., GREGERSEN, B. A., LOPEZ, X., DE LERA, A. R., AND YORK, D. M. Pseudorotation of Natural and Chemically Modified Biological Phosphoranes: Implications for RNA Catalysis. *Chem. Phys. Chem.* **5** (2004), 1045–1049.

(3) MAYAAN, E., MOSER, A., JR., A. D. M., AND YORK, D. M. CHARMM Force Field Parameters for Simulation of Reactive Intermediates in Native and Thio-Substituted Ribozymes. *J. Comput. Chem.* **28** (2007), 495–507.

(4) LIU, Y., GREGERSEN, B. A., LOPEZ, X., AND YORK, D. M. Density Functional Study of the In-Line Mechanism of Methanolysis of Cyclic Phosphate and Thiophosphate Esters in Solution: Insight into Thio Effects in RNA Transesterification. *J. Phys. Chem. B* **109** (2005), 19987–20003.

(5) GIESE, T. J., GREGERSEN, B. A., LIU, Y., NAM, K., MAYAAN, E., MOSER, A., RANGE, K., NIETO FAZA, O., SILVA LOPEZ, C., RODRIGUEZ DE LERA, A., SCHAFTENAAR, G., LOPEZ, X., LEE, T., KARYPIS, G., AND YORK, D. M. QCRNA 1.0: A database of quantum calculations of RNA catalysis. *J. Mol. Graph. Model.* **25** (2006), 423–433.

(6) PONOMAREV, S. Y., THAYER, K. M., AND BEVERIDGE, D. L. Ion motions in molecular dynamics simulations on DNA. *Proc. Natl. Acad. Sci. USA* **101** (2004), 14771–14775.

(7) MARTICK, M. AND SCOTT, W. G. Tertiary contacts distant from the active site prime a ribozyme for catalysis. *Cell* **126** (2006), 309–320.